Tetherin inhibits Nipah virus but not Ebola virus replication in fruit bat cells

Markus Hoffmann[1], Inga Nehlmeier[1], Constantin Brinkmann[1,2], Verena Krähling[3], Laura Behner[3], Anna-Sophie Moldenhauer[1], Nadine Krüger[4,5], Julia Nehls[6,7], Michael Schindler[6,7], Thomas Hoenen[8], Andrea Maisner[3], Stephan Becker[3], Stefan Pöhlmann[1,2]

Infection Biology Unit, German Primate Center, Kellnerweg 4, 37077 Göttingen, Germany[1]; Faculty of Biology and Psychology, University Göttingen, Wilhelm-Weber-Str. 2, 37073 Göttingen, Germany[2]; Institute of Virology, Philipps-University Marburg, Hans-Meerwein-Straße 2, 35043 Marburg, Germany[3], Institute of Virology, University of Veterinary Medicine Hannover, 30559 Hannover, Germany[4]; Research Center for Emerging Infections and Zoonoses, University of Veterinary Medicine Hannover, 30559 Hannover, Germany[5]; Institute of Medical Virology and Epidemiology of Viral Diseases, University Hospital Tübingen, 72076 Tübingen, Germany[6]; Institute of Virology, Helmholtz Center Munich – Research Center for Environmental Health, 85764 Neuherberg, Germany[7]; Institute of Molecular Virology and Cell Biology, Friedrich-Loeffler-Institut, Greifswald, Insel Riems, Germany[8]

Address correspondence to Markus Hoffmann, mhoffmann@dpz.eu, or Stefan Pöhlmann, spoehlmann@dpz.eu

ABSTRACT

Ebola virus (EBOV) and Nipah virus (NiV) infection of humans can cause fatal disease and constitutes a public health threat. In contrast, EBOV and NiV infection of fruit bats, the putative (EBOV) or proven (NiV) natural reservoir, is not associated with disease and it is currently unknown how these animals control the virus. The human interferon (IFN)-stimulated antiviral effector protein tetherin (CD317, BST-2) blocks release of EBOV- and NiV-like particles from cells and is counteracted by the EBOV glycoprotein (GP). In contrast, it is unknown whether fruit bat tetherin restricts virus infection and is susceptible to GP-driven antagonism. Here, we report the sequence of fruit bat tetherin and show that its expression is IFN-stimulated and associated with strong antiviral activity. Moreover, we demonstrate that EBOV-GP antagonizes tetherin orthologues of diverse species but fails to efficiently counteract fruit bat tetherin in virus-like particle (VLP) release assays. However, unexpectedly, tetherin was dispensable for robust IFN-mediated inhibition of EBOV spread in fruit bat cells. Thus, the VLP-based model system mimicking tetherin-mediated inhibition of EBOV release and its counteraction by GP seems not to adequately reflect all aspects of EBOV release from IFN-stimulated fruit bat cells, potentially due to differences in tetherin expression levels that could not be resolved by the present study. In contrast, tetherin expression was essential for IFN-dependent inhibition of NiV infection, demonstrating that IFN-induced fruit bat tetherin exerts antiviral activity and may critically contribute to control of NiV and potentially other highly virulent viruses in infected animals.

IMPORTANCE

Ebola virus and Nipah virus (EBOV, NiV) can cause fatal disease in humans. In contrast, infected fruit bats do not develop symptoms but can transmit the virus to humans. Why fruit bats but not humans control infection is largely unknown. Tetherin is an antiviral host cell protein and is counteracted by the EBOV glycoprotein in human cells. Here, employing model systems, we show that tetherin of fruit bats displays higher antiviral activity than human tetherin and is largely resistant against counteraction by the Ebola virus glycoprotein. Moreover, we demonstrate that induction of tetherin expression is critical for interferon-mediated inhibition of NiV but, for at present unknown reasons, not EBOV spread in fruit bat cells. Collectively, our findings identify tetherin as an antiviral effector of innate immune responses in fruit bats, which might allow these animals to control infection with NiV and potentially other viruses that cause severe disease in humans.

KEY WORDS

Ebola virus, Nipah virus, tetherin, reservoir, fruit bat

INTRODUCTION

Ebola virus (EBOV), a member of the *Filoviridae*, is highly virulent in humans and non-human primates. The devastating Ebola virus disease (EVD) epidemic in West Africa claimed more than 11.000 lives (1, 2) and the frequent introduction of the virus into the human population from animal reservoirs during the last decades and its persistence in infected patients (3-5) suggest that similar outbreaks can occur at any time. Moreover, no approved vaccines or therapeutics are available to combat EBOV at present, although testing of certain vaccines in clinical trials yielded encouraging results (6). Thus, EBOV constitutes a serious health threat and the development of novel countermeasures is called for.

Nipah virus (NiV), a zoonotic paramyxovirus, was first recognized during an outbreak of fatal encephalitis and pneumonia in pig farmers and abattoir workers in Malaysia and Singapore in 1998 (7-9). Since 2001, NiV has caused multiple independent outbreaks in Bangladesh, India and (potentially) the Philippines (10-15), resulting in more than 600 cases of which more than half had a fatal outcome. Finally, as for EBOV, neither approved vaccines nor therapeutics are available to combat NiV infection, highlighting that NiV is an unmet threat to public health in South-East Asia.

Asian fruit bats of the genus *Pteropus* are the natural reservoir of NiV (16-18) and may transmit the virus directly to humans or via pigs, which can serve as intermediate hosts (9, 10). (12, 13, 19). African fruit bats are believed to be the natural reservoir of EBOV for which several outbreaks have been associated with contact of humans with bats (20-23). Analysis of naturally and experimentally infected fruit bats revealed that these animals amplify NiV and EBOV but do not develop disease (20-25). Therefore, understanding how fruit bats control infection by these two viruses might help to define novel targets for antiviral intervention. Recent studies suggest

that fruit bats might be equipped with a constitutively active interferon (IFN) system (26), which might constitute a powerful defense against viral spread. IFN can inhibit virus infection by inducing the expression of IFN-stimulated genes (ISGs), many of which encode products with antiviral activity (27). However, it is incompletely understood which ISG-encoded proteins restrict EBOV and NiV infection of human cells. Moreover, EBOV and NiV restricting factors (termed restriction factors) in fruit bat cells have not been identified, although inhibition of an EBOV mini-replicon by bat Mx proteins in transfected human cells has been reported (28).

The tetherin protein (CD317, BST-2) is an IFN-induced restriction factor that can block spread of several enveloped viruses by preventing release of progeny particles from infected cells (29-31). Tetherin can exert its antiviral activity due to the presence of two membrane anchors, an N-terminal transmembrane domain and a C-terminal glycosylphosphatidylinositol (GPI) anchor. These elements allow tetherin to simultaneously insert into viral and cellular membranes, thereby forming a physical tether between the cell surface and virus particles (32). Human immunodeficiency virus type 1 (HIV-1) and several other viruses encode tetherin antagonizing proteins which interfere with appropriate tetherin expression and/or cellular localization and thus allow viral spread in tetherin-positive cells (30, 31, 33).

The glycoprotein (GP) of EBOV mediates viral entry into target cells and rescues release of VP40-based particles from inhibition by tetherin (34), using a poorly understood mechanism. Inhibition of EBOV release by tetherin has so far only been observed in the context of surrogate systems and formally it remains to be demonstrated that tetherin inhibits viral release and is counteracted by GP in the context of EBOV infected cells. Nevertheless, two studies reported that release of EBOV from infected cells is not blocked by human tetherin (35, 36), suggesting that GP-dependent tetherin antagonism might help the virus to evade control by the human IFN

system. In contrast, the contribution of tetherin to the innate defenses of fruit bats against EBOV is unknown. Similarly, little information is available regarding the role of tetherin in NiV infection. Two studies reported that release of NiV-like particles, produced by directed expression of the NiV matrix protein, is reduced when tetherin is coexpressed (36, 37). However, it is unknown whether the NiV surface glycoproteins F and G, like EBOV-GP, can antagonize tetherin and whether tetherin is able to restrict spread of authentic NiV.

Here, we report that expression of fruit bat tetherin is stimulated by IFN and show that the protein efficiently restricts release of EBOV-like particles from cells. Furthermore, we reveal that EBOV-GP fails to efficiently antagonize fruit bat tetherin upon directed expression. Finally, we provide evidence that tetherin is essential for efficient IFN-mediated inhibition of fruit bat cell infection by vesicular stomatitis virus (VSV), a prototype RNA virus from the *Rhabdoviridae* family, and NiV, while, unexpectedly, EBOV spread in fruit bat cells was only moderately affected by tetherin.

RESULTS

EBOV-GP antagonizes human, non-human primate, rodent and artificial tetherin. We first investigated whether EBOV-GP can antagonize tetherin orthologues of diverse species, including non-human primate and rodent tetherin as well as artificial tetherin, which has no sequence homology with human tetherin (32). For this, we employed a previously described HIV-1 Gag-based virus-like particle (VLP) release assay (35), which is commonly used in the field. All tetherin proteins tested in this assay reduced release of VLPs (Fig. 1A and B). The HIV-1 Vpu protein, a prototypic tetherin antagonist, counteracted human and the closely related gorilla tetherin but was largely inactive against the other tetherin orthologues tested (Fig. 1C), in agreement with previous findings (38, 39). In contrast, EBOV-GP counteracted the antiviral activity of all tetherin proteins tested, including artificial tetherin (Fig. 1C). These findings, which confirm and extend a previous report (40), indicate a broad and potentially sequence independent anti-tetherin activity of EBOV-GP.

Fruit bat tetherin is a potent antiviral factor. We next investigated whether tetherin orthologues from an assumed EBOV-reservoir, *Hypsignathus monstrosus* (21), and a related fruit bat species, *Epomops buettikoferi*, can inhibit VLP release and are susceptible to EBOV-GP-mediated antagonism. For this, we PCR-amplified and cloned the complete tetherin open-reading frames from EpoNi/22.1 (*E. buettikoferi*, Epo) and HypNi/1.1 (*H. monstrosus*, Hyp) cells. Sequence analysis showed that both fruit bat tetherins cluster phylogenetically with predicted tetherin proteins of bats and that human and fruit bat tetherin display an identical domain organization, including conserved cysteine residues and N-glycosylation motifs (Fig. 2A and B).

We next asked whether the similarities in sequence (human/Hyp, 46.7%; human/Epo, 46.2%) and domain organization between human and fruit bat tetherins resulted in comparable expression and antiviral activity. Both fruit bat tetherins showed increased formation of higher order multimers (Fig. 3A) and Epo tetherin was less efficiently N-glycosylated (Fig. 3B) as compared to human tetherin but no appreciably differences in the subcellular localization of human and Epo tetherin were observed (Fig. 3C). Total expression (immunoblot) of fruit bat tetherins exceeded that of human tetherin by about 2-fold (Fig. 3D and F). However, total expression of fruit bat tetherins was less efficient than that observed for several other tetherin orthologues shown to be susceptible to counteraction by EBOV-GP, including murine (Fig. 1C, present study) and porcine tetherin (41) (Fig. 3D). Importantly, human and fruit bat tetherin were comparably expressed at the cell surface (flow cytometry, Fig. 3E and F; surface levels of tetherins examined in figure 1 were not determined), indicating that human and fruit bat tetherin are equally well expressed at the place where tetherin unfolds its antiviral activity.

Both human and fruit bat tetherin proteins robustly interfered with release of HIV-1 Gag- and EBOV-VP40-based particles (Fig. 4A-D), and release of the latter is believed to adequately mirror important aspects of release of EBOV from infected cells. Moreover, both fruit bat tetherins exhibited higher resistance against counteraction by HIV-1 Vpu than human tetherin (Fig. 4A-D). Notably, Epo tetherin was also largely resistant against counteraction by EBOV-GP under the conditions chosen while resistance of Hyp tetherin was less pronounced. In keeping with these findings, both fruit bat tetherins were more potent than human tetherin in inhibiting the release of replication-competent EBOV-like particles in a system that, unlike the VP40-based particles studied above, faithfully mimics most steps of EBOV infection (42) (Fig. 4E). Finally, resistance of fruit bat tetherin to counteraction by EBOV-GP was dependent on the amount of

tetherin plasmid transfected and thus on tetherin expression levels (not shown). Collectively, these results indicate that fruit bat tetherins, like human tetherin, are potent antiviral factors that can be largely resistant to counteraction by EBOV-GP when expressed at high levels.

Endogenous expression of fruit bat tetherin is induced by IFN and inhibits VSV infection.

All previously discussed results were obtained upon directed expression of tetherin. Therefore, we asked whether endogenous fruit bat tetherin also exerts antiviral activity. To this end, we first examined whether EpoNi/22.1 (established from kidney of *E. buettikoferi*) and HypNi/1.1 cells (established from kidney of *H. monstrosus)* (43, 44), from which tetherin was cloned, as well as other fruit bat cell lines were responsive to treatment with pan IFNα. Human A549 cells were included as positive control, since these cells are known to be highly IFN-sensitive. Treatment of all cell lines with IFN at non-cytotoxic concentrations (data not shown) markedly reduced transduction by a single-cycle VSV vector in a concentration-dependent manner (Fig. 5A). Since IFN-mediated reduction of transduction was more prominent for EpoNi/22.1 (inhibitory concentration 50 [IC50] = 2.34 U/ml) as compared to HypNi/1.1 cells (IC50 = 4.99 U/ml, respectively), the former cell line was selected for subsequent analyses. Quantitative RT-PCR, using myxovirus resistance protein 1 (*Mx1*) as positive control for IFN-stimulated gene expression, showed that tetherin mRNA expression was highly upregulated in A549 cells upon IFN treatment (Fig. 5B), as expected. Similarly, IFN stimulation upregulated tetherin mRNA levels in EpoNi/22.1 cells, although not to the same extent as *Mx1* encoding mRNA (Fig. 5B). Thus, fruit bat cells transit into an antiviral state upon IFN treatment and tetherin expression is induced by IFN in these cells, allowing us to determine whether tetherin contributes to the antiviral effect of IFN treatment. For this, we utilized a replication-competent VSV variant

209 encoding eGFP, since this virus is known to be highly IFN-sensitive. Indeed, treatment of A549
210 and EpoNi/22.1 cells with IFN decreased VSV infection (Fig. 5C) and reduced production of
211 progeny virus by more than 100,000-fold (for A549 cells, mean titers dropped from ~1.6 x 10^9
212 ffu/ml to ~2.9 x 10^4 ffu/ml upon IFN-stimulation, while for EpoNi/22.1 cells titers dropped from
213 ~7.5 x 10^8 ffu/ml to ~5.5 x 10^3 ffu/ml upon IFN-stimulation) (Fig. 5D). Using this system in
214 conjunction with siRNA-mediated gene knockdown, we next asked whether tetherin contributes
215 to the IFN-mediated antiviral state. The IFN-induced block of infection of A549 cells was
216 modestly (~5-fold) rescued upon pre-treatment of cells with siRNA against human tetherin (mean
217 titer: ~1.3 x 10^4 ffu/ml) compared to cells treated with control siRNA (mean titer: ~6.4 x 10^4
218 ffu/ml) (Fig. 5C and E), suggesting that expression of other ISGs can facilitate efficient inhibition
219 of VSV in the absence of tetherin in this cell line. More strikingly, siRNAs against fruit bat
220 tetherin but not nonsense control siRNA reduced tetherin mRNA expression (Fig. 5F) and
221 strongly (~150-fold) rescued the generation of infectious VSV in fruit bat cells (mean titers: ~1.3
222 x 10^3 ffu/ml [control siRNA] and ~1.9 x 10^5 ffu/ml [tetherin-specific siRNA]) (Fig. 5E). The
223 rescue most likely occurred at the stage of viral release, the target of tetherins antiviral activity,
224 since transduction, genome transcription and translation of virally encoded proteins in IFN-
225 treated cells were not impacted by the siRNA (Fig, 5G). In sum, our results indicate that tetherin
226 expression in fruit bat cells is IFN-inducible and is to a significant part responsible for the IFN-
227 mediated blockade of VSV infection.
228
229 **Fruit bat tetherin is required for efficient inhibition of NiV but not EBOV infection by IFN.**
230 In light of the important contribution of tetherin to control of VSV infection in fruit bat cells, we
231 investigated whether tetherin also contributes to the blockade of EBOV and NiV infection by

IFN. NiV was included in the analysis, since the virus uses fruit bats as natural reservoir (18), is highly pathogenic in humans and may be tetherin-sensitive. Thus, tetherin was previously shown to inhibit release of NiV-like particles (36, 37) and analysis of the viral surface proteins, NiV-F and NiV-G, revealed that they do not antagonize tetherin (Fig. 6A and B). IFN pretreatment reduced EBOV and NiV spread in EpoNi/22.1 cells by roughly 20- and 30-fold, respectively (Fig. 6C-E). For NiV, transfection of tetherin siRNA rescued this blockade almost entirely as it increased titers of free virus in the culture supernatant by ~20-fold (Fig. 6D and F). In contrast, EBOV spread was only slightly rescued (~2-fold) (Fig. 6C and F).These findings suggest that tetherin may be a major contributor to control of NiV infection in fruit bats, the natural reservoir, while tetherin's contribution to inhibition of EBOV spread in the natural reservoir might be moderate.

DISCUSSION

Fruit bats, the suspected natural reservoir of EBOV and the proven reservoir of NiV, control EBOV and NiV infection by poorly understood means, although a contribution of the IFN system has been suspected (26). Here, we show that expression of fruit bat-encoded tetherin is IFN-stimulated and associated with robust antiviral activity. Moreover, we demonstrate that fruit bat tetherin critically contributes to IFN-dependent control of VSV and NiV but not EBOV infection of fruit bat cells.

The antiviral activity of tetherin was first reported by Neil and colleagues in the context of HIV-1 infection (30) but it is now well established that tetherin can also inhibit the spread of several other enveloped viruses (31, 33). Tetherin can exert a broad antiviral activity because it targets a host cell-derived component of virions, the viral envelope. The EBOV-GP was shown to counteract tetherin and to promote release of VP40-based VLPs from transfected cells (34). Moreover, two reports demonstrated that human tetherin expression does not appreciably inhibit spread of authentic EBOV (35, 36), indicating that GP-mediated tetherin antagonism might allow for viral amplification in tetherin-positive cells. However, the contribution of tetherin to viral control in the natural reservoir has not been examined.

Our results show that tetherin from *E. buettikoferi* and *H. monstrosus* share ~46% sequence identity with human tetherin. Moreover, the fruit bat tetherin orthologues (99.5% sequence identity) contain all functional elements previously defined for human tetherin: An N-terminal cytoplasmic domain, a transmembrane domain, an extracellular coiled coil region, a C-terminal GPI anchor, two sequons for attachment of N-glycans and three cysteines available for formation of disulfide bonds. Moreover, fruit bat tetherin orthologues and human tetherin showed a roughly comparable cellular localization, with both proteins being detectable in the

endoplasmic reticulum, Golgi apparatus, trans-Golgi network, recycling endosomes and at the cell surface. Strikingly, however, tetherins from *E. buettikoferi* and, to a lesser degree, *H. monstrosus* were, in contrast to human tetherin, largely resistant against EBOV-GP-mediated counteraction, at least under conditions of high expression. This finding is noteworthy considering that EBOV-GP antagonizes tetherin orthologues of diverse species, as evidenced by the present study and published work (35, 40), and is even active against artificial tetherin (40). At present, it is unclear why fruit bat tetherin was resistant against EBOV-GP counteraction under the conditions chosen. However, it is noteworthy the fruit bat tetherin was barely N-glycosylated in 293T cells and the role of tetherin N-glycosylation in resistance deserves further investigation.

The robust antiviral activity of fruit bat tetherin in transfected cells raised the question whether endogenous tetherin contributes to viral control in fruit bat cells. After identification of EpoNi/22.1 cells as being responsive to IFN-treatment using a single-cycle VSV vector, quantitative PCR revealed that tetherin mRNA was upregulated upon IFN treatment, indicating that fruit bat tetherin like its human counterpart is an ISG. Strikingly, IFN stimulation combined with siRNA knockdown showed that tetherin was essential for robust IFN-mediated inhibition of VSV and NiV but not EBOV infection of fruit bat cells. The observation that NiV spread was sensitive to fruit bat tetherin expression is in keeping with the published finding that release of NiV-like particles is inhibited by human tetherin (36, 37) and the new finding that NiV-F and NiV-G fail to antagonize tetherin, at least in a HIV Gag-based assay. However, the major contribution of tetherin to IFN-mediated control of NiV infection is remarkable, since exposure of human and likely also fruit bat cells to IFN stimulates the expression of several hundred genes, many of which encode proteins which exert antiviral activity (27). An explanation for the

moderate contribution of fruit bat tetherin to IFN-mediated control of EBOV spread might reside in tetherin expression levels. Resistance of fruit bat tetherin to counteraction by EBOV-GP in VLP assays was dependent on the amount of tetherin plasmid transfected and it is conceivable that tetherin expression levels attained upon IFN stimulation of cells might have been insufficient to provide resistance against EBOV-GP-mediated counteraction. Resolving this question requires reagents that allow comparing fruit bat tetherin levels on the surface of transfected and IFN treated cells, which are not available at present. Furthermore, the possibility, although remote, that authentic EBOV (unlike VP40-based EBOV particles) might be intrinsically tetherin resistant should not be discarded. This scenario can only be investigated upon identification of mutations in GP that selectively interfere with tetherin antagonism and first steps in this direction have recently been made (45).

Collectively, our findings show that tetherin is central to the IFN-mediated control of NiV in fruit bat cells while the factor(s) required for the robust control of EBOV in these animals (26, 46) remain to be elucidated.

MATERIALS AND METHODS

Cells and viruses. HEK-293T (human, kidney) and A549 (human, lung) cells were cultivated in Dulbecco's Modified Eagle Medium (DMEM, Pan) and DMEM/F-12 medium (Gibco), respectively, supplemented with 10% fetal bovine serum (FBS, Biochrom) and penicillin/streptomycin (PAN) at a final concentration of 100 units/ml (penicillin) and 0.1 µg/ml (streptomycin). Vero E6, Vero76 (both African green monkey, kidney) and BHK-21 (Syrian hamster, kidney) cells were cultivated in DMEM supplemented with 5% FBS and penicillin/streptomycin. The following fruit bat cell lines, a kind gift of C. Drosten and M. A. Müller, were cultivated in DMEM supplemented with 10% FBS and penicillin/streptomycin: EpoNi/22.1 (Buettikofer's epauletted fruit bat, *Epomops buettikoferi*; kidney), HypNi/1.1 (Hammer-headed fruit bat, *Hypsignathus monstrosus*; kidney), RoNi/7 (Egyptian fruit bat, *Rousettus aegyptiacus*; kidney), EidNi/41 and EidLu/43 (Straw-colored fruit bat, *Eidolon helvum*; kidney and lung, respectively). For subcultivation and seeding, cells were washed with phosphate-buffered saline (PBS) and detached by incubation in a trypsin/EDTA solution (PAN) or by resuspension in DMEM (293T). Cell numbers were determined under a light microscope using a Neubauer chamber. Cultivation of cells was carried out at 37°C in humidified atmosphere containing 5% CO_2.

We employed a recombinantly produced vesicular stomatitis virus (VSV, Indiana strain), which expresses enhanced green fluorescent protein (eGFP) from an additional transcription unit located between the open-reading frames (ORF) for the viral glycoprotein (G) and RNA-dependent RNA-polymerase (L). The Ebola virus strain Zaire, Mayinga (GenBank accession number: NC_002549) used in the study was propagated in Vero E6 cells, virus titer was

347 determined by immunoplaque titration. Furthermore, we utilized a Nipah virus (NiV, Malaysia
348 strain) that contains an eGFP transcription unit between the NiV-G and NiV-L ORFs and that has
349 been described elsewhere (47).
350
351 **Cloning of fruit bat tetherin.** Total cellular RNA was isolated from ~10^6 HypNi/1.1 (Hyp) and
352 EpoNi/22.1 (Epo) cells using the RNeasy mini kit (Qiagen) according to the manufacturer's
353 protocol. Next, 1 µg RNA was used as a template for cDNA synthesis employing the
354 SuperScript® III First-Strand Synthesis System (ThermoFisher Scientific) according to the
355 manufacturer's protocol (for random hexamers). A fragment of ~550 bp was amplified using
356 Phusion polymerase (ThermoFisher Scientific). Primers were designed based on predicted fruit
357 bat tetherin sequences from the NCBI (National Center for Biotechnology Information) database
358 as template (primer sequences available upon request). Next, the DNA fragments were separated
359 by agarose gel electrophoresis, extracted from the gel by commercial kits (Macherey & Nagel)
360 and inserted into the pCAGGS expression vector using the EcoRI and XhoI sites. Upon
361 transformation into competent *E. coli* by heat-shock, three individual clones, which contained the
362 insert, were subjected to automated sequence analysis (SeqLab). Sequences of Epo and Hyp
363 tetherin have been submitted to GenBank and are available under the accession numbers
364 MG792836 and MG792837, respectively.
365
366 **Plasmids, mutagenesis and transfection.** Expression plasmids for human immunodeficiency
367 virus (HIV-) 1 p55-Gag (Gag), HIV-1 Vpu (Vpu), the glycoprotein of Ebola virus (EBOV-GP),
368 VSV (VSV-G), Nipah virus fusion (F) and attachment glycoprotein (G), EBOV-VP40 harboring
369 an N-terminal cMYC tag, and DC-SIGN have been described elsewhere (35, 44, 48-50). To

generate expression plasmids for human, gorilla, African green monkey, pig, rat, mouse and artificial tetherin, the respective ORFs were amplified from existing plasmids (32, 51, 52) and inserted into the pCAGGS expression vector. Rhesus macaque and marmoset tetherin were PCR-amplified from reverse-transcribed lung RNA as described for fruit bat tetherin and inserted into the pCAGGS expression vector. Additionally, tetherin constructs were equipped with an N-terminal HA (YPYDVPDYA) epitope and identity of all PCR-amplified sequences was verified by automated sequence analysis (SeqLab). For the detection of tetherin at the cell surface via flow cytometry, human and fruit bat tetherin constructs with an extracellular HA epitope (located upstream of their respective GPI-anchor motifs) were cloned. Furthermore, eGFP-based expression vectors for localization studies targeting the endoplasmic reticulum (ER), Golgi apparatus (both kindly provided by F. van Kuppeveld, (9), trans-Golgi network (TGN, TGN integral membrane protein 2) and Rab10- or Rab11a-positive recycling endosomes were used. We further employed a previously described transcription and replication-competent EBOV-like particle system that included pCAGGS-driven expression plasmids for T7-polymerase, EBOV-NP, -VP35, -VP30 and -L, and a plasmid-coded minigenome that contains the genetic information for Renilla luciferase (RLuc) as a reporter gene (42). Plasmid transfection of 293T cells was carried out by calcium phosphate precipitation, while Vero76 cells were transfected using ICAFectin441 (In-Cell-Art).

Analysis of tetherin expression and virus-like particle (VLP) release assays. Expression of tetherin was analyzed by transfection of 293T cells grown in 12-well plates with expression plasmids for different tetherin constructs (2 µg). The impact of tetherin and EBOV-GP on the release of Gag- or VP40-based VLPs was studied essentially as described elsewhere (35, 49).

293T cells grown in 12-well plates were cotransfected with combinations of expression plasmids for Gag or VP40 (2 µg), tetherin (0.5 µg) and potential antagonist (2 µg). As controls and for equilibration of total DNA amounts, empty pCAGGS expression vector or an eGFP expression plasmid were used. At 16 h post transfection, the transfection medium was replaced by fresh culture medium and cells were incubated for an additional 32 h. Then, supernatants were collected, cleared from cellular debris by centrifugation and VLPs were pelleted from cleared supernatants by high-speed centrifugation through a 20% sucrose cushion. Next, 50 µl of 2 x SDS loading buffer were added to concentrated VLPs and samples were incubated at 95°C for 30 min before being directly used for analysis or stored at -20°C until further use. In parallel, whole cell lysates (WCL) were prepared by first washing cells with PBS and then lysing them with 100 µl 2x SDS-containing lysis buffer (30 mM Tris/pH 6.8, 10% glycerol, 2% SDS, 5% β-mercaptoethanol, 0.1% bromophenol blue, 1 mM EDTA). After 15 min of incubation at room temperature, samples were incubated at 95°C for 30 min and either directly used for analysis or stored at -20°C until further use.

Quantification of VLP-release. Quantification of Gag and VP40 release was carried out using the program ImageJ (FIJI distribution) (53). For this, Gag or VP40 signals detected in the supernatants (corresponding to VLPs) were normalized against the respective signals obtained in WCL. For comparison of multiple samples (e.g. different tetherin orthologues or tetherin antagonists), one sample was set at 100% and designated as reference (i.e. Gag or VP40 release in the absence of tetherin and antagonist) for all other samples in that experiment. At least three independent immunoblots were used for quantification.

SDS-polyacrylamide gel electrophoresis (SDS-PAGE) and immunoblot analysis. VLP and WCL samples were separated via SDS-PAGE using gels containing 12.5% polyacrylamide and transferred onto a nitrocellulose membrane (GE Lifesciences, 0.2 µm) using a tank blot system (Bio-Rad). Following blotting, membranes were blocked in 5% milk powder in PBS containing 0.1% Tween 20 (PBS-T) for 1 h at room temperature before antibody incubation was performed as follows: HIV-1 Gag was detected using supernatant of hybridoma cells secreting a mouse anti-Gag antibody (183-H12-5C) at a dilution of 1:100, while EBOV-VP40 containing an N-terminal cMYC tag was detected using supernatant of hybridoma cells secreting a mouse anti-cMYC antibody (9E10) at a dilution of 1:3. For detection of tetherin containing an HA epitope, an HA-specific mouse antibody (Sigma-Aldrich) was employed at a dilution of 1:1,000. Primary antibody binding was further detected through incubation with an anti-mouse, horseradish peroxidase (HRP-) coupled secondary antibody (Dianova) at a dilution of 1:10,000. Visualization of bound secondary antibodies was achieved using a self-made ECL solution (0.1 M Tris-HCl pH 8.6, 250 µg/ml luminol, 1 mg/ml para-hydroxycoumaric acid, 0.3% H_2O_2) in combination with the ChemoCam imaging system and the ChemoStarProfessional software (Intas). After imaging of the Gag, VP40 and tetherin signals in WCL, membranes were stripped of bound antibodies by incubation with stripping buffer (12.5% 0.5 M Tris/HCl, pH 6.8; 2% SDS; 0.8% ß-mercaptoethanol) for 30 min at 50°C, rinsed with running water for 1 h, washed with PBS-T and re-blocked. Subsequently, membranes were probed with ß-actin-specific rabbit (1:1,000; Sigma-Aldrich) and rabbit-specific, HRP-conjugated secondary antibodies (1:10,000; Dianova) for detection of ß-actin levels as a loading control.

438 **Production of transcription and replication-competent EBOV-like particles (trVLPs) and**
439 **transduction of target cells.** To assess the impact of tetherin expression on the EBOV-like
440 particles, we employed a tetracistronic transcription and replication-competent virus-like particle
441 (trVLP) system that resembles many aspects of the EBOV life cycle (42). Briefly, 293T cells
442 grown in 6-well plates were cotransfected with expression plasmids for EBOV-NP (125 ng), -
443 VP35 (125 ng), -VP30 (75 ng) -L (1 µg), p4cis-vRNA-RLuc (250 ng), T7-polymerase (250 ng),
444 and tetherin or empty expression vector as control (500 ng) (= producer cells). At 16 h post
445 transfection, the transfection medium was replaced by fresh culture medium and cells were
446 incubated for an additional 56 h. Then, supernatants were collected, cleared from cellular debris
447 by centrifugation and trVLPs were inoculated onto 293T cells grown in 96-well plates that were
448 previously (24 h) cotransfected with EBOV-NP (25 ng), -VP35 (25 ng), -VP30 (15 ng) -L (200
449 µg) and DC-SIGN (250 ng) (= target cells). Target cells were further incubated for 72 h. In order
450 to investigate the ability of tetherin to restrict spread of trVLPs in both producer and target cells,
451 cells were lysed in 50 µl/well (target cells) or 100 µl/well (producer cells) cell culture lysis
452 reagent (Promega). Next, lysates were transferred into white, opaque-walled 96-well plates,
453 incubated with an in house-made RLuc substrate and RLuc activity was measured in a microplate
454 reader (Hidex).
455
456 **Flow cytometry.** Analysis of tetherin expression at the cell surface was performed as follows:
457 293T cells were transfected with human or fruit bat tetherin harboring an extracellular HA
458 epitope. Cells transfected with an eGFP expression vector or empty plasmid served as negative
459 controls. At 48 h post transfection, cells were washed and resuspended in PBS supplemented with
460 0.1% BSA (Roth, PBS/BSA). Next, samples were split into two reaction tubes and probed either

with an HA-epitope specific mouse antibody (Sigma-Aldrich) or an isotype control antibody (Sigma-Aldrich, 1:100) for 1 h at 4°C. Subsequently, cells were pelleted, washed with PBS/BSA and incubated with an AlexaFluor647-coupled anti-mouse antibody (ThermoFisher Scientific, 1:100), again for 1 h at 4°C. Afterwards, cells were washed 2x with PBS/BSA, fixed with 2% paraformaldehyde and staining was analyzed employing a LSR II Flow Cytometer in combination with the FACS Diva software (both BD Biosciences). Further data analysis was performed using the FCS Express 4 Flow research software (De Novo software).

Phylogenetic and sequence analyses. Phylogenetic analysis was performed utilizing the MEGA 6 (version 6.06) software package (54). For this, sequences were aligned (MUSCLE algorithm) and a phylogenetic tree was constructed based on the neighbor-joining method with 1,000 bootstrap iterations. Amino acid sequences of diverse mammalian tetherin orthologues were obtained from the NCBI database and are summarized in Table S1. For motif and domain predictions, the following online tools were used: HMMTOP (http://www.enzim.hu/hmmtop/, transmembrane domains), NetNGlyc 1.0 (http://www.cbs.dtu.dk/services/NetNGlyc/, N-glycosylation motifs), Coiled-Coil Prediction (https://npsa-prabi.ibcp.fr/cgi-bin/npsa_automat.pl?page=npsa_lupas.html, coiled-coil domains) and big-PI Predictor (http://mendel.imp.ac.at/gpi/gpi_server.html, GPI-anchor addition sites).

Transduction with single-cycle VSV vectors. We employed a previously described, replication-deficient VSV that lacks the genetic information for VSV-G but instead harbors separate transcription units encoding eGFP and firefly luciferase (FLuc), VSV*ΔG-FLuc (kindly provided by G. Zimmer) (12). Propagation of VSV*ΔG-FLuc and trans-complementation with VSV-G was

484 achieved on a helper cell line that expresses VSV-G in an inducible fashion, BHK-21(G43) (55).
485 To quantify FLuc activity upon inoculation of cells with VSV*ΔG-FLuc, cell culture
486 supernatants were removed and cells washed with PBS followed by cell lysis using the Cell
487 Culture Lysis Reagent (Promega) for 30 min. Subsequently, lysates were transferred into white,
488 opaque-walled 96-well plates. Finally, FLuc substrate (PJK) was added and luminescence signals
489 were detected using a plate luminometer (Hidex).
490
491 **Knockdown of endogenous tetherin expression by siRNA.** Human tetherin-specific siRNA
492 and the corresponding control siRNA-A were purchased from Santa Cruz, while custom-designed
493 stealth siRNA specific for fruit bat tetherin and the corresponding medium GC-content control
494 siRNA were obtained from ThermoFisher Scientific. Delivery of siRNA into A549, HypNi/1.1
495 and EpoNi/22.1 cells (25 pmol/well, 12-well format) was achieved using RNAiMAX
496 (ThermoFisher Scientific) according to the manufacturer's protocol.
497
498 **Quantification of tetherin transcripts by quantitative PCR (qPCR).** In order to measure
499 mRNA transcripts levels for tetherin, *Mx1* (interferon-stimulated gene control) and ß-actin
500 (housekeeping gene control) upon siRNA-transfection and/or pan-IFNα-stimulation, quantitative
501 PCR (qPCR) of reverse-transcribed total cellular RNA was employed. First, RNA was extracted
502 from cells using the RNeasy mini kit (Qiagen) according to manufacturer's protocol. Next, 1 µg
503 RNA was treated with DNase I (New England Biolabs) to eliminate co-isolated genomic DNA
504 and directly used as a template for cDNA synthesis employing the SuperScript® III First-Strand
505 Synthesis System (ThermoFisher Scientific) according to the manufacturer's protocol (for
506 random hexamers). Thereafter, 1 µl of cDNA mix were subjected to qPCR on a Rotorgene Q

platform (Qiagen) using the QuantiTect SYBR Green PCR Kit (Qiagen) with primers targeting either human or fruit bat tetherin (designed using the Genescript online tool, https://www.genscript.com/tools/real-time-pcr-tagman-primer-design-tool), *Mx1* or ß-actin (14). Induction of tetherin and *Mx1* gene expression following stimulation with pan-IFNα (displayed as expression fold change) was analyzed by the 2-ΔΔCt-method (15) with ß-actin as housekeeping gene. To assess the efficiency of siRNA-mediated knockdown by qPCR, relative tetherin transcript levels for control siRNA-treated, pan-IFNα-stimulated cells was set as 100% and compared to the value for cells transfected with siRNA targeting tetherin and stimulated with pan-IFNα.

Infection of cells with replication-competent VSV, EBOV or NiV. All experiments with live EBOV and NiV were performed under biosafety level 4 (BSL-4) conditions at the Institute of Virology, Philipps University Marburg by trained personnel and in accordance with national regulations. After removal of the cell culture supernatant, cells were washed one time and subsequently inoculated with VSV (MOI = 0.005), EBOV or NiV (both MOI = 0.1). All experiments were performed in 12-well format in triplicates and mock-infected cells served as controls. At 1 h p.i, cells were washed and further incubated with fresh culture medium. Viral titers in the supernatant were quantified at 1 h (all viruses, washing control) and 24 h (VSV) or 48 h (EBOV, NiV) p.i..

Quantification of viral titers. VSV titers were quantified on confluently grown BHK-21 cells (96-well format) that were inoculated with 10-fold serial dilutions of the supernatants to be analyzed. At 1 h p.i., cells were overlaid with culture medium containing 1% methylcellulose

530 (Sigma-Aldrich) to only allow viral spread between neighboring cells, resulting in focus
531 formation. At 18 h p.i., eGFP-positive foci were counted under the fluorescence microscope
532 (focus forming units per ml, ffu/ml). To quantify the relative inhibition of virus replication by
533 stimulation with pan-IFNα, the x-fold difference between VSV titers in supernatants of mock-
534 versus pan-IFNα-treated cells was calculated. In addition, the relative rescue of VSV from
535 tetherin restriction by siRNA-mediated tetherin knockdown in pan-IFNα-treated cells was
536 quantified by calculating the x-fold difference between VSV titers in supernatants of control
537 versus tetherin-specific siRNA-transfected cells. EBOV and NiV titers were analyzed on Vero E6
538 and Vero76 cells, respectively, inoculated with 10-fold serial dilutions of the supernatants. At 5
539 d. p.i. (NiV) or 14 d. p.i. (EBOV), the tissue culture infectious dose 50 per ml (TCID50/ml) was
540 calculated based on the formation of cytopathic effects and employing the Spearman-Kärber
541 method (47, 56).
542
543 **Fluorescence microscopy.** To analyze intracellular localization of human and fruit bat tetherin,
544 Vero76 cells grown on coverslips were cotransfected with expression plasmids for tetherin
545 constructs harboring an N-terminal HA-epitope and the respective marker for the ER, Golgi,
546 TGN, or Rab10- or Rab11a-positive recycling endosomes, all linked to eGFP, using
547 ICAFectin441 (In-Cell-Art) as transfection reagent according to the manufacturer's protocol. At
548 24 h post transfection, cells were fixed, permeabilized with 0.1% Triton-X-100 in PBS and
549 subsequently incubated with anti-HA (Sigma-Aldrich, 1:500) and anti-mouse AlexaFluor594
550 (ThermoFisher Scientific, 1:500) antibodies. Finally, cells were incubated with DAPI (Roth) to
551 stain cellular nuclei and coverslips were mounted on glass slides using Mowiol containing
552 DABCO (Roth) as anti-bleaching reagent. Representative pictures were taken at a magnification

of 100x using a Nikon Eclipse Ti fluorescence microscope in combination with the NIS elements AR software (both Nikon). To investigate VSV spread in cells transfected with control or tetherin-specific siRNA and subsequently treated with or without pan-IFNα, cells were fixed at 24 h p.i. and pictures were taken at a magnification of 10x.

ACKNOWLEDGEMENTS

This work was funded by Deutsche Forschungsgemeinschaft (DFG), grants PO 716/8-1 (to S.P.), SCHI1073/4-1 (to M.S.), SFB 1021, B04 (to A.M). and SFB 1021, A02 (to S.B.). In addition, this work was funded by German Federal Ministry of Education and Research (BMBF), EBOKON consortium (S.P., S.B.). The funders had no role in the design of the research and the interpretation of the research results. We would like to thank F. van Kuppeveld, G. Sutter, G. Zimmer, and C. Drosten and M. A. Müller for reagents. The authors like to thank F. van Kuppeveld, G. Zimmer, and C. Drosten and M. A. Müller for providing the eGFP-tagged markers for the ER and Golgi apparatus, the replication-deficient VSV vector, and the fruit bat cell lines, respectively.

REFERENCES

1. **WHO.** Ebola Situation Report - 17 February 2016. http://apps.who.int/ebola/current-situation/ebola-situation-report-17-february-2016. 17-2-2016.

2. **WHO Ebola Response Team**. 2016. Ebola Virus Disease among Male and Female Persons in West Africa. N. Engl. J. Med. **374**:96-98.

3. **Biava, M., C. Caglioti, L. Bordi, C. Castilletti, F. Colavita, S. Quartu, E. Nicastri, F. N. Lauria, N. Petrosillo, S. Lanini, T. Hoenen, G. Kobinger, A. Zumla, C. A. Di, G. Ippolito, M. R. Capobianchi, and E. Lalle**. 2017. Detection of Viral RNA in Tissues following Plasma Clearance from an Ebola Virus Infected Patient. PLoS. Pathog. **13**:e1006065.

4. **Brainard, J., K. Pond, L. Hooper, K. Edmunds, and P. Hunter**. 2016. Presence and Persistence of Ebola or Marburg Virus in Patients and Survivors: A Rapid Systematic Review. PLoS. Negl. Trop. Dis. **10**:e0004475.

5. **Deen, G. F., B. Knust, N. Broutet, F. R. Sesay, P. Formenty, C. Ross, A. E. Thorson, T. A. Massaquoi, J. E. Marrinan, E. Ervin, A. Jambai, S. L. McDonald, K. Bernstein, A. H. Wurie, M. S. Dumbuya, N. Abad, B. Idriss, T. Wi, S. D. Bennett, T. Davies, F. K. Ebrahim, E. Meites, D. Naidoo, S. Smith, A. Banerjee, B. R. Erickson, A. Brault, K. N. Durski, J. Winter, T. Sealy, S. T. Nichol, M. Lamunu, U. Stroher, O. Morgan, and F. Sahr**. 2015. Ebola RNA Persistence in Semen of Ebola Virus Disease Survivors - Preliminary Report. N. Engl. J. Med.

6. **Martins, K. A., P. B. Jahrling, S. Bavari, and J. H. Kuhn**. 2016. Ebola virus disease candidate vaccines under evaluation in clinical trials. Expert. Rev. Vaccines. **15**:1101-1112.

7. **Centers of Disease Control**. 1999. From the Centers for Disease Control and Prevention. Outbreak of Hendra-like virus--Malaysia and Singapore, 1998-1999. JAMA **281**:1787-1788.

8. **Paton, N. I., Y. S. Leo, S. R. Zaki, A. P. Auchus, K. E. Lee, A. E. Ling, S. K. Chew, B. Ang, P. E. Rollin, T. Umapathi, I. Sng, C. C. Lee, E. Lim, and T. G. Ksiazek**. 1999. Outbreak of Nipah-virus infection among abattoir workers in Singapore. Lancet **354**:1253-1256.

9. **Chua, K. B., K. J. Goh, K. T. Wong, A. Kamarulzaman, P. S. Tan, T. G. Ksiazek, S. R. Zaki, G. Paul, S. K. Lam, and C. T. Tan**. 1999. Fatal encephalitis due to Nipah virus among pig-farmers in Malaysia. Lancet **354**:1257-1259.

10. **Chadha, M. S., J. A. Comer, L. Lowe, P. A. Rota, P. E. Rollin, W. J. Bellini, T. G. Ksiazek, and A. Mishra**. 2006. Nipah virus-associated encephalitis outbreak, Siliguri, India. Emerg. Infect. Dis. **12**:235-240.

11. **Ching, P. K., V. C. de los Reyes, M. N. Sucaldito, E. Tayag, A. B. Columna-Vingno, F. F. Malbas, Jr., G. C. Bolo, Jr., J. J. Sejvar, D. Eagles, G. Playford, E. Dueger, Y. Kaku, S. Morikawa, M. Kuroda, G. A. Marsh, S. McCullough, and A. R. Foxwell**. 2015. Outbreak of henipavirus infection, Philippines, 2014. Emerg. Infect. Dis. **21**:328-331.

12. **Gurley, E. S., J. M. Montgomery, M. J. Hossain, M. Bell, A. K. Azad, M. R. Islam, M. A. Molla, D. S. Carroll, T. G. Ksiazek, P. A. Rota, L. Lowe, J. A. Comer, P. Rollin, M. Czub, A. Grolla, H. Feldmann, S. P. Luby, J. L. Woodward, and R. F. Breiman**. 2007. Person-to-person transmission of Nipah virus in a Bangladeshi community. Emerg. Infect. Dis. **13**:1031-1037.

13. **Islam, M. S., H. M. Sazzad, S. M. Satter, S. Sultana, M. J. Hossain, M. Hasan, M. Rahman, S. Campbell, D. L. Cannon, U. Stroher, P. Daszak, S. P. Luby, and E. S. Gurley**. 2016. Nipah Virus Transmission from Bats to Humans Associated with Drinking Traditional Liquor Made from Date Palm Sap, Bangladesh, 2011-2014. Emerg. Infect. Dis. **22**:664-670.

14. **Lo, M. K., L. Lowe, K. B. Hummel, H. M. Sazzad, E. S. Gurley, M. J. Hossain, S. P. Luby, D. M. Miller, J. A. Comer, P. E. Rollin, W. J. Bellini, and P. A. Rota**. 2012. Characterization of Nipah virus from outbreaks in Bangladesh, 2008-2010. Emerg. Infect. Dis. **18**:248-255.

15. **Luby, S. P., M. J. Hossain, E. S. Gurley, B. N. Ahmed, S. Banu, S. U. Khan, N. Homaira, P. A. Rota, P. E. Rollin, J. A. Comer, E. Kenah, T. G. Ksiazek, and M. Rahman**. 2009. Recurrent zoonotic transmission of Nipah virus into humans, Bangladesh, 2001-2007. Emerg. Infect. Dis. **15**:1229-1235.

16. **Chua, K. B., C. L. Koh, P. S. Hooi, K. F. Wee, J. H. Khong, B. H. Chua, Y. P. Chan, M. E. Lim, and S. K. Lam**. 2002. Isolation of Nipah virus from Malaysian Island flying-foxes. Microbes. Infect. **4**:145-151.

17. **Rahman, S. A., S. S. Hassan, K. J. Olival, M. Mohamed, L. Y. Chang, L. Hassan, N. M. Saad, S. A. Shohaimi, Z. C. Mamat, M. S. Naim, J. H. Epstein, A. S. Suri, H. E. Field, and P. Daszak**. 2010. Characterization of Nipah virus from naturally infected Pteropus vampyrus bats, Malaysia. Emerg. Infect. Dis. **16**:1990-1993.

18. **Yob, J. M., H. Field, A. M. Rashdi, C. Morrissy, B. van der Heide, P. Rota, A. A. bin, J. White, P. Daniels, A. Jamaluddin, and T. Ksiazek**. 2001. Nipah virus infection in bats (order Chiroptera) in peninsular Malaysia. Emerg. Infect. Dis. **7**:439-441.

19. **Rahman, M. A., M. J. Hossain, S. Sultana, N. Homaira, S. U. Khan, M. Rahman, E. S. Gurley, P. E. Rollin, M. K. Lo, J. A. Comer, L. Lowe, P. A. Rota, T. G. Ksiazek, E.**

Kenah, Y. Sharker, and S. P. Luby. 2012. Date palm sap linked to Nipah virus outbreak in Bangladesh, 2008. Vector. Borne. Zoonotic. Dis. **12**:65-72.

20. **Hayman, D. T., P. Emmerich, M. Yu, L. F. Wang, R. Suu-Ire, A. R. Fooks, A. A. Cunningham, and J. L. Wood**. 2010. Long-term survival of an urban fruit bat seropositive for Ebola and Lagos bat viruses. PLoS. One. **5**:e11978.

21. **Leroy, E. M., B. Kumulungui, X. Pourrut, P. Rouquet, A. Hassanin, P. Yaba, A. Delicat, J. T. Paweska, J. P. Gonzalez, and R. Swanepoel**. 2005. Fruit bats as reservoirs of Ebola virus. Nature **438**:575-576.

22. **Leroy, E. M., A. Epelboin, V. Mondonge, X. Pourrut, J. P. Gonzalez, J. J. Muyembe-Tamfum, and P. Formenty**. 2009. Human Ebola outbreak resulting from direct exposure to fruit bats in Luebo, Democratic Republic of Congo, 2007. Vector. Borne. Zoonotic. Dis. **9**:723-728.

23. **Ogawa, H., H. Miyamoto, E. Nakayama, R. Yoshida, I. Nakamura, H. Sawa, A. Ishii, Y. Thomas, E. Nakagawa, K. Matsuno, M. Kajihara, J. Maruyama, N. Nao, M. Muramatsu, M. Kuroda, E. Simulundu, K. Changula, B. Hang'ombe, B. Namangala, A. Nambota, J. Katampi, M. Igarashi, K. Ito, H. Feldmann, C. Sugimoto, L. Moonga, A. Mweene, and A. Takada**. 2015. Seroepidemiological Prevalence of Multiple Species of Filoviruses in Fruit Bats (Eidolon helvum) Migrating in Africa. J. Infect. Dis. **212 Suppl 2**:S101-S108.

24. **Paweska, J. T., N. Storm, A. A. Grobbelaar, W. Markotter, A. Kemp, and v. Jansen, V**. 2016. Experimental Inoculation of Egyptian Fruit Bats (Rousettus aegyptiacus) with Ebola Virus. Viruses. **8**.

25. **Middleton, D. J., C. J. Morrissy, B. M. van der Heide, G. M. Russell, M. A. Braun, H. A. Westbury, K. Halpin, and P. W. Daniels**. 2007. Experimental Nipah virus infection in pteropid bats (Pteropus poliocephalus). J. Comp Pathol. **136**:266-272.

26. **Zhou, P., M. Tachedjian, J. W. Wynne, V. Boyd, J. Cui, I. Smith, C. Cowled, J. H. Ng, L. Mok, W. P. Michalski, I. H. Mendenhall, G. Tachedjian, L. F. Wang, and M. L. Baker**. 2016. Contraction of the type I IFN locus and unusual constitutive expression of IFN-alpha in bats. Proc. Natl. Acad. Sci. U. S. A **113**:2696-2701.

27. **Schoggins, J. W., S. J. Wilson, M. Panis, M. Y. Murphy, C. T. Jones, P. Bieniasz, and C. M. Rice**. 2011. A diverse range of gene products are effectors of the type I interferon antiviral response. Nature **472**:481-485.

28. **Fuchs, J., M. Holzer, M. Schilling, C. Patzina, A. Schoen, T. Hoenen, G. Zimmer, M. Marz, F. Weber, M. A. Muller, and G. Kochs**. 2017. Evolution and Antiviral Specificities of Interferon-Induced Mx Proteins of Bats against Ebola, Influenza, and Other RNA Viruses. J. Virol. **91**.

29. **Neil, S. J., V. Sandrin, W. I. Sundquist, and P. D. Bieniasz**. 2007. An interferon-alpha-induced tethering mechanism inhibits HIV-1 and Ebola virus particle release but is counteracted by the HIV-1 Vpu protein. Cell Host. Microbe **2**:193-203.

30. **Neil, S. J., T. Zang, and P. D. Bieniasz**. 2008. Tetherin inhibits retrovirus release and is antagonized by HIV-1 Vpu. Nature **451**:425-430.

31. **Neil, S. J.** 2013. The antiviral activities of tetherin. Curr. Top. Microbiol. Immunol. **371**:67-104.

32. **Perez-Caballero, D., T. Zang, A. Ebrahimi, M. W. McNatt, D. A. Gregory, M. C. Johnson, and P. D. Bieniasz**. 2009. Tetherin inhibits HIV-1 release by directly tethering virions to cells. Cell **139**:499-511.

33. **Sauter, D.** 2014. Counteraction of the multifunctional restriction factor tetherin. Front Microbiol. **5**:163.

34. **Kaletsky, R. L., J. R. Francica, C. Agrawal-Gamse, and P. Bates**. 2009. Tetherin-mediated restriction of filovirus budding is antagonized by the Ebola glycoprotein. Proc. Natl. Acad. Sci. U. S. A **106**:2886-2891.

35. **Kühl, A., C. Banning, A. Marzi, J. Votteler, I. Steffen, S. Bertram, I. Glowacka, A. Konrad, M. Sturzl, J. T. Guo, U. Schubert, H. Feldmann, G. Behrens, M. Schindler, and S. Pöhlmann**. 2011. The Ebola virus glycoprotein and HIV-1 Vpu employ different strategies to counteract the antiviral factor tetherin. J. Infect. Dis. **204 Suppl 3**:S850-S860.

36. **Radoshitzky, S. R., L. Dong, X. Chi, J. C. Clester, C. Retterer, K. Spurgers, J. H. Kuhn, S. Sandwick, G. Ruthel, K. Kota, D. Boltz, T. Warren, P. J. Kranzusch, S. P. Whelan, and S. Bavari**. 2010. Infectious Lassa virus, but not filoviruses, is restricted by BST-2/tetherin. J. Virol. **84**:10569-10580.

37. **Kong, W. S., T. Irie, A. Yoshida, R. Kawabata, T. Kadoi, and T. Sakaguchi**. 2012. Inhibition of virus-like particle release of Sendai virus and Nipah virus, but not that of mumps virus, by tetherin/CD317/BST-2. Hiroshima J. Med. Sci. **61**:59-67.

38. **Kobayashi, T., H. Ode, T. Yoshida, K. Sato, P. Gee, S. P. Yamamoto, H. Ebina, K. Strebel, H. Sato, and Y. Koyanagi**. 2011. Identification of amino acids in the human tetherin transmembrane domain responsible for HIV-1 Vpu interaction and susceptibility. J. Virol. **85**:932-945.

39. **McNatt, M. W., T. Zang, T. Hatziioannou, M. Bartlett, I. B. Fofana, W. E. Johnson, S. J. Neil, and P. D. Bieniasz**. 2009. Species-specific activity of HIV-1 Vpu and positive selection of tetherin transmembrane domain variants. PLoS. Pathog. **5**:e1000300.

40. **Lopez, L. A., S. J. Yang, H. Hauser, C. M. Exline, K. G. Haworth, J. Oldenburg, and P. M. Cannon**. 2010. Ebola virus glycoprotein counteracts BST-2/Tetherin restriction in

a sequence-independent manner that does not require tetherin surface removal. J. Virol. **84**:7243-7255.

41. **Brinkmann, C., M. Hoffmann, A. Lubke, I. Nehlmeier, A. Kramer-Kuhl, M. Winkler, and S. Pöhlmann**. 2017. The glycoprotein of vesicular stomatitis virus promotes release of virus-like particles from tetherin-positive cells. PLoS. One. **12**:e0189073.

42. **Watt, A., F. Moukambi, L. Banadyga, A. Groseth, J. Callison, A. Herwig, H. Ebihara, H. Feldmann, and T. Hoenen**. 2014. A novel life cycle modeling system for Ebola virus shows a genome length-dependent role of VP24 in virus infectivity. J. Virol. **88**:10511-10524.

43. **Hoffmann, M., M. A. Muller, J. F. Drexler, J. Glende, M. Erdt, T. Gutzkow, C. Losemann, T. Binger, H. Deng, C. Schwegmann-Wessels, K. H. Esser, C. Drosten, and G. Herrler**. 2013. Differential sensitivity of bat cells to infection by enveloped RNA viruses: coronaviruses, paramyxoviruses, filoviruses, and influenza viruses. PLoS. One. **8**:e72942.

44. **Hoffmann, M., H. M. Gonzalez, E. Berger, A. Marzi, and S. Pöhlmann**. 2016. The Glycoproteins of All Filovirus Species Use the Same Host Factors for Entry into Bat and Human Cells but Entry Efficiency Is Species Dependent. PLoS. One. **11**:e0149651.

45. **Gonzalez-Hernandez, M., M. Hoffmann, C. Brinkmann, J. Nehls, M. Winkler, M. Schindler, and S. Pöhlmann**. 2018. A GXXXA Motif in the Transmembrane Domain of the Ebola Virus Glycoprotein Is Required for Tetherin Antagonism. J. Virol. **92**.

46. **Kuzmin, I. V., T. M. Schwarz, P. A. Ilinykh, I. Jordan, T. G. Ksiazek, R. Sachidanandam, C. F. Basler, and A. Bukreyev**. 2017. Innate Immune Responses of Bat and Human Cells to Filoviruses: Commonalities and Distinctions. J. Virol. **91**.

47. **Dietzel, E., L. Kolesnikova, B. Sawatsky, A. Heiner, M. Weis, G. P. Kobinger, S. Becker, M. von, V, and A. Maisner**. 2015. Nipah Virus Matrix Protein Influences Fusogenicity and Is Essential for Particle Infectivity and Stability. J. Virol. **90**:2514-2522.

48. **Brinkmann, C., I. Nehlmeier, K. Walendy-Gnirss, J. Nehls, H. M. Gonzalez, M. Hoffmann, X. Qiu, A. Takada, M. Schindler, and S. Pöhlmann**. 2016. The Tetherin Antagonism of the Ebola Virus Glycoprotein Requires an Intact Receptor-Binding Domain and Can Be Blocked by GP1-Specific Antibodies. J. Virol. **90**:11075-11086.

49. **Gnirss, K., M. Fiedler, A. Kramer-Kuhl, S. Bolduan, E. Mittler, S. Becker, M. Schindler, and S. Pöhlmann**. 2014. Analysis of determinants in filovirus glycoproteins required for tetherin antagonism. Viruses. **6**:1654-1671.

50. **Lamp, B., E. Dietzel, L. Kolesnikova, L. Sauerhering, S. Erbar, H. Weingartl, and A. Maisner**. 2013. Nipah virus entry and egress from polarized epithelial cells. J. Virol. **87**:3143-3154.

51. **Goffinet, C., I. Allespach, S. Homann, H. M. Tervo, A. Habermann, D. Rupp, L. Oberbremer, C. Kern, N. Tibroni, S. Welsch, J. Krijnse-Locker, G. Banting, H. G. Krausslich, O. T. Fackler, and O. T. Keppler**. 2009. HIV-1 antagonism of CD317 is species specific and involves Vpu-mediated proteasomal degradation of the restriction factor. Cell Host. Microbe **5**:285-297.

52. **Sauter, D., M. Schindler, A. Specht, W. N. Landford, J. Munch, K. A. Kim, J. Votteler, U. Schubert, F. Bibollet-Ruche, B. F. Keele, J. Takehisa, Y. Ogando, C. Ochsenbauer, J. C. Kappes, A. Ayouba, M. Peeters, G. H. Learn, G. Shaw, P. M. Sharp, P. Bieniasz, B. H. Hahn, T. Hatziioannou, and F. Kirchhoff**. 2009. Tetherin-driven adaptation of Vpu and Nef function and the evolution of pandemic and nonpandemic HIV-1 strains. Cell Host. Microbe **6**:409-421.

53. **Schindelin, J., I. Arganda-Carreras, E. Frise, V. Kaynig, M. Longair, T. Pietzsch, S. Preibisch, C. Rueden, S. Saalfeld, B. Schmid, J. Y. Tinevez, D. J. White, V. Hartenstein, K. Eliceiri, P. Tomancak, and A. Cardona**. 2012. Fiji: an open-source platform for biological-image analysis. Nat. Methods **9**:676-682.

54. **Tamura, K., G. Stecher, D. Peterson, A. Filipski, and S. Kumar**. 2013. MEGA6: Molecular Evolutionary Genetics Analysis version 6.0. Mol. Biol. Evol. **30**:2725-2729.

55. **Hanika, A., B. Larisch, E. Steinmann, C. Schwegmann-Wessels, G. Herrler, and G. Zimmer**. 2005. Use of influenza C virus glycoprotein HEF for generation of vesicular stomatitis virus pseudotypes. J. Gen. Virol. **86**:1455-1465.

56. **Krähling, V., D. Becker, C. Rohde, M. Eickmann, Y. Eroglu, A. Herwig, R. Kerber, K. Kowalski, J. Vergara-Alert, and S. Becker**. 2016. Development of an antibody capture ELISA using inactivated Ebola Zaire Makona virus. Med. Microbiol. Immunol. **205**:173-183.

811 **FIGURE LEGENDS**

812

813 FIG 1 EBOV-GP antagonizes tetherin orthologues from diverse species. (A) HEK-293T cells
814 were transfected with expression plasmids for HIV-1 Gag and the indicated tetherin orthologues,
815 artificial tetherin or empty plasmid as control. The release of Gag-derived virus-like particles
816 (VLPs) in culture supernatants and Gag expression in whole cell lysates (WCL) were analyzed by
817 immunoblot. Expression of ß-actin was determined as loading control. A representative blot is
818 shown from which irrelevant lanes were excised. (B) The average of four experiments conducted
819 as described for panel A and quantified via the ImageJ program is shown. The release of Gag in
820 the absence of tetherin was set as 100%. Error bars indicate the standard error of the mean
821 (SEM). One-way ANOVA with Bonferroni post-test analysis was performed to test statistical
822 significance (**, $p \leq 0.005$; ***, $p \leq 0.001$). (C) The release assay was conducted as described
823 for panel A but the tetherin antagonists HIV-1 Vpu and EBOV-GP were included. The results of
824 a representative blot are shown and were confirmed in a separate experiment.

825

826 FIG 2 Fruit bat tetherin and human tetherin exhibit the same domain organization. (A)
827 Phylogenetic relationship of mammalian tetherin proteins (see Table S1 for additional
828 information): Protein sequences of tetherin proteins from the indicated species were aligned and a
829 phylogenetic tree was constructed using MEGA 6 (version 6.06). Small numbers at the nodes
830 reflect bootstrap values and the scale bar indicates the number of amino acid substitutions per site
831 (for simplicity, only values above 80 are shown). Black circles indicate the fruit bat species of
832 which tetherin proteins were investigated in the present study. The identifiers “X1” and “X2”
833 refer to different isoforms present in the NCBI database. (B) Domain organization (top) and

834 sequence alignment of fruit bat and human tetherin. Conserved cysteine residues (red, asterisks),
835 glycosylation motifs (blue, sticks and circles), GPI-anchor (black arrowhead, grey box) and the
836 only amino acid variation between the two fruit bat tetherins studied (position 174, glycine or
837 serine; orange box) are indicated. CD, cytoplasmic domain; TD, transmembrane domain.
838
839 FIG 3 Fruit bat tetherin displays similar subcellular localization and surface expression as human
840 tetherin. (A) Expression of human and fruit bat tetherin in transfected HEK-293T cells was
841 analyzed by immunoblot (amounts of expression plasmids were adjusted to allow for comparable
842 expression levels). An antibody directed against an N-terminal HA antigenic tag added to the
843 tetherin orthologues was used for detection of tetherin expression. Expression of ß-actin was
844 determined as loading control. Similar results were obtained in a separate experiment. Hyp
845 (*Hypsignathus. monstrosus*), Epo (*Epomops buettikoferi*). Red (human) and blue (fruit bat)
846 arrowheads indicate unglycosylated (open arrowheads), partially glycosylated (dashed
847 arrowheads) and fully glycosylated (filled arrowheads) tetherin, respectively, while asterisks
848 mark multimeric forms. (B) Cell lysates of HEK-293T cells transfected with human or fruit bat
849 (Epo) tetherin were either untreated or treated with PNGase F to enzymatically remove potential
850 N-glycans and subsequently analyzed by immunoblot (as described for panel A). A representative
851 blot is shown and similar results were obtained in two separate experiments. (C) Vero76 cells
852 were cotransfected with identical amounts of expression plasmids coding for human or fruit bat
853 tetherin (containing an N-terminal HA-tag) and marker proteins for either the endoplasmic
854 reticulum (ER), Golgi apparatus (Golgi), trans-Golgi network (TGN), or Rab10- or Rab11a-
855 positive recycling endosomes (all fused to eGFP). At 24 h post transfection, cells were fixed,
856 permeabilized, and subsequently incubated with an HA-specific primary antibody and

857 AlexaFluor594-labelled secondary antibody. Finally, cellular nuclei were stained with DAPI and
858 samples were processed for fluorescence microscopy. Shown are representative pictures at 100-
859 fold magnification with all fluorescence channels merged into one picture. Similar results were
860 obtained a separate experiment. (D) Identical amounts of expression plasmids for the indicated
861 tetherin orthologues equipped with an N-terminal HA-epitope were transfected into HEK-293T
862 cells and tetherin expression in whole cell lysates was investigated by Western blot analysis,
863 using an HA-specific antibody. Cells transfected with empty expression vector served as control.
864 Similar results were obtained in two separate experiments. (E) The experiment was performed as
865 described for panel C but human and fruit bat tetherin proteins with an HA tag within the
866 extracellular domain (located upstream of the GPI-anchoring signal) were used and tetherin
867 expression was analyzed by flow cytometry. The average of eight independent experiments is
868 shown for which geometric mean channel fluorescence measured for cells expressing human
869 tetherin was set as 1. Error bars indicate SEM. Statistical significance was analyzed by one-way
870 ANOVA with Bonferroni posttest analysis (ns, $p > 0.05$). (F). Normalized data from experiments
871 examining tetherin expression in whole cell lysates (WCL, immunoblot, $n = 7$) and at the cell
872 surface (Surface, flow cytometry, $n = 8$) are shown. Expression of human tetherin was set as one
873 and expression of fruit bat tetherin was calculated as x-fold changes +/- SEM.
874
875 FIG 4 Fruit bat tetherin is largely resistant against counteraction by EBOV-GP. (A) HEK-293T
876 cells were cotransfected with expression plasmids for Gag, human tetherin or the indicated
877 tetherin orthologues, and tetherin antagonist (Vpu, EBOV-GP). Cells transfected with empty
878 expression vector instead of tetherin and /or antagonist served as controls. The release of Gag-
879 derived virus-like particles (VLPs) in culture supernatants and Gag expression in whole cell

880 lysates (WCL) was analyzed by immunoblot. Expression of ß-actin was determined as loading
881 control. (B) The average of four experiments conducted as described for panel A and quantified
882 via the ImageJ program is shown. The release of Gag in the absence of tetherin and antagonist
883 was set as 100%. Error bars indicate SEM. (C) The release assay was conducted as described for
884 panel A, but EBOV-VP40 was used instead of HIV-1-Gag. Detection of VP40 was carried out
885 using an antibody targeting the N-terminal cMYC tag. (D) The average of six experiments
886 conducted as described for panel C and quantified via the ImageJ program is shown. The release
887 of VP40 in the absence of tetherin and antagonist was set as 100%. Error bars indicate SEM. (E)
888 Transcription and replication-competent virus-like particles (trVLP system) were produced in
889 293T cells in the absence or presence of the indicated tetherin proteins and used to transduce
890 fresh 293T cells expressing DC-SIGN and the EBOV polymerase complex (EBOV-NP, -VP35, -
891 VP30, -L). Activity of *Renilla* luciferase, encoded by the viral mini-genome, as an indicator for
892 trVLP infection was measured . For normalization, luciferase activity for trVLP produced in the
893 absence of tetherin was set as 100%. Presented are the combined results from three independent
894 experiments with error bars indicating SEM. Statistical significance of the data presented in
895 panels B, D and E was tested by one-way ANOVA with Bonferroni posttest analysis (ns, $p > 0.05$; *, $p \leq 0.05$; **, $p \leq 0.01$; ***, $p \leq 0.001$).
896
897
898 FIG 5 Expression of fruit bat tetherin is IFN-inducible and required for robust IFN-mediated
899 inhibition of VSV infection. (A) The indicated fruit bat cell lines were incubated with increasing
900 amounts of pan-IFNα, inoculated with a single-cycle VSV vector bearing VSV-G and encoding
901 luciferase (VSV*ΔG-FLuc) and luciferase activity in cell lysates was quantified. Luciferase
902 activity measured for cells treated with medium without pan-IFNα was set as 100%. The results

903 of a representative experiment performed with triplicate samples are shown and were confirmed
904 in a separate experiment. Error bars indicate SEM. The inhibitory concentration 50, IC50, was
905 calculated for each cell line and is indicated. (B) Human (A549) and fruit bat (EpoNi/22.1) cells
906 were pan-IFNα- or mock-treated, cellular RNA was extracted, reverse transcribed into cDNA and
907 analyzed for transcript levels of ß-actin, *Mx1* (myxovirus resistance protein) and tetherin by
908 quantitative PCR (qRT-PCR). Shown are combined data (given as expression fold change upon
909 IFN-treatment, normalized to β-actin) of three independent experiments. Error bars indicate
910 SEM. (C) Human (A549) and fruit bat (EpoNi/22.1) cells were transfected with the indicated
911 siRNAs (ns, nonsense = control) or left untransfected and then either treated with pan-IFNα- or
912 mock-treated, followed by inoculation with replication competent VSV encoding eGFP. Finally,
913 infected cells (as determined by expression of eGFP) were detected via fluorescence microscopy.
914 Similar results were obtained in five separate experiments. (D) Viral titers in the cellular
915 supernatants of the untransfected, IFNα- or mock-treated cells described in panel C were
916 quantified. The relative (x-fold) differences between viral titers in the supernatants of pan-IFNα-
917 and mock-treated cells were calculated. The average of six independent experiments performed
918 with triplicate samples is shown. Error bars indicate the SEM. (E) Viral titers in the cellular
919 supernatants of the siRNA-transfected and IFN-treated cells described in panel C were quantified.
920 The relative (x-fold) differences between viral titers of pan-IFNα-treated cells transfected with
921 control or tetherin-specific siRNA were calculated. The average of six independent experiments
922 performed with triplicate samples is shown. Error bars indicate the SEM. (F) Relative tetherin
923 transcript levels in IFN-treated fruit bat cells (EpoNi/22.1), which were previously transfected
924 with either control (ns) or fruit bat tetherin-specific (batTetherin) siRNA, were compared by
925 qRT-PCR (normalized against ß-actin transcript levels). Shown are the combined results of three

926 independent experiments performed with triplicate samples, in which tetherin transcript levels of
927 IFN-treated cells that received control siRNA were set as 100%. Error bars indicate SEM. (G)
928 Human (A549) and fruit bat (EpoNi/22.1) cells were transfected with no-targeting (control) or
929 tetherin-specific siRNA prior to treatment with pan-IFNα. At 48 h post transfection, cells were
930 inoculated with single-cycle VSV vector pseudotyped with VSV-G (VSV*ΔG-FLuc). After an
931 incubation period of 1 h, cells were washed and further incubated for 8 h, before virus-encoded
932 luciferase activity was quantified in cell lysates. Shown are normalized data of three independent
933 experiments performed with quadruplicate samples in which transduction of cells without prior
934 IFN-treatment was set as 100%. Error bars indicate SEM. Statistical significance of the data
935 presented in panels D and E were analyzed using the Mann-Whitney-U test, while the data
936 presented in panels F and G were analyzed by paired, two-tailed students t-test (ns, $p > 0.05$; **,
937 $p \leq 0.01$).
938
939 FIG 6 Fruit bat tetherin is required for robust IFN-mediated inhibition of NiV but not EBOV
940 spread. (A) HEK-293T cells were cotransfected with expression plasmids for Gag, human
941 tetherin and HIV-1-Vpu, EBOV-GP, NiV-F, NiV-G or NiV-F+G. Cells transfected with empty
942 expression plasmid instead of tetherin and/or (potential) antagonist served as controls. The
943 release of Gag-derived virus-like particles (VLPs) in culture supernatants and Gag expression in
944 whole cell lysates (WCL) was analyzed by immunoblot. Expression of ß-actin was determined as
945 loading control. (B) The average of three experiments conducted as described for panel A and
946 quantified via the ImageJ program is shown. The release of Gag in the absence of tetherin was set
947 as 100%. Error bars indicate SEM. (C,D) EpoNi/22.1 cells that were transfected with control (ns)
948 or fruit bat tetherin-specific siRNA (batT) and subsequently treated with pan-IFNα- or mock-

949 treated were inoculated with EBOV (C) or NiV (D). Subsequently, the cells were washed,
950 incubated and viral titers in culture supernatants quantified by measuring the tissue culture
951 infectious dose 50 per ml (TCID50/ml). Panels C and D show the mean and individual titers for
952 all experimental conditions measured in four independent experiments (performed with triplicate
953 samples). Error bars indicate SEM. (E) The data from panels C and D were used to calculate the
954 relative (x-fold) reduction of viral spread upon IFN treatment. The combined data from four
955 independent experiments performed with triplicate samples are shown. Error bars indicate SEM.
956 (F) The data from panels C and D were used to calculate the relative (x-fold) differences between
957 viral titers in the supernatants of pan-IFNα-treated cells that were transfected with either control
958 or tetherin-specific siRNA. The combined data from four independent experiments performed
959 with triplicate samples are shown. Error bars indicate SEM. Statistical significance of the data
960 presented in panel B were analyzed by one-way ANOVA with Bonferroni posttest analysis, while
961 the data presented in panels E and F were analyzed using the Mann-Whitney-U test (ns, $p > 0.05$;
962 *, $p \leq 0.05$; ***, $p \leq 0.001$).
963
964
965
966

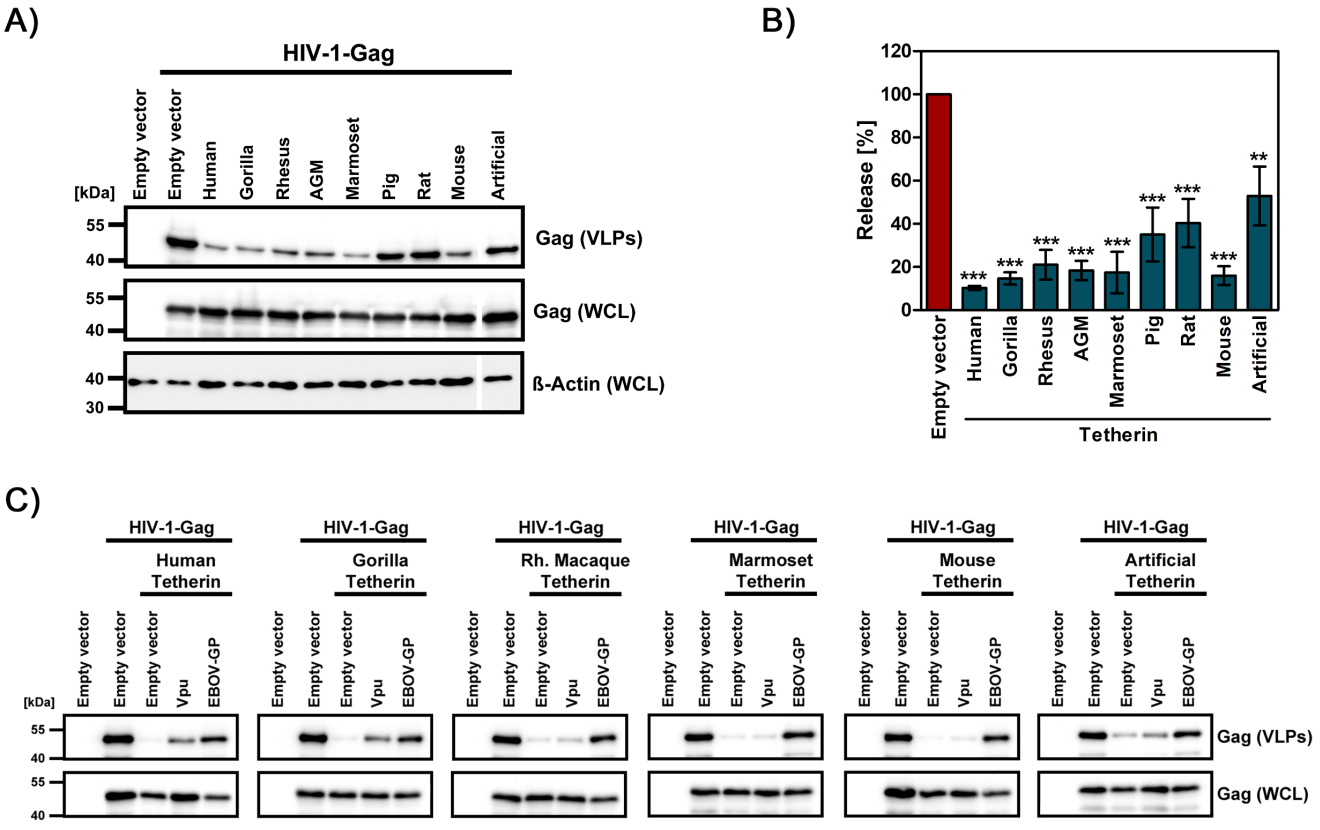

Figure 2

A)

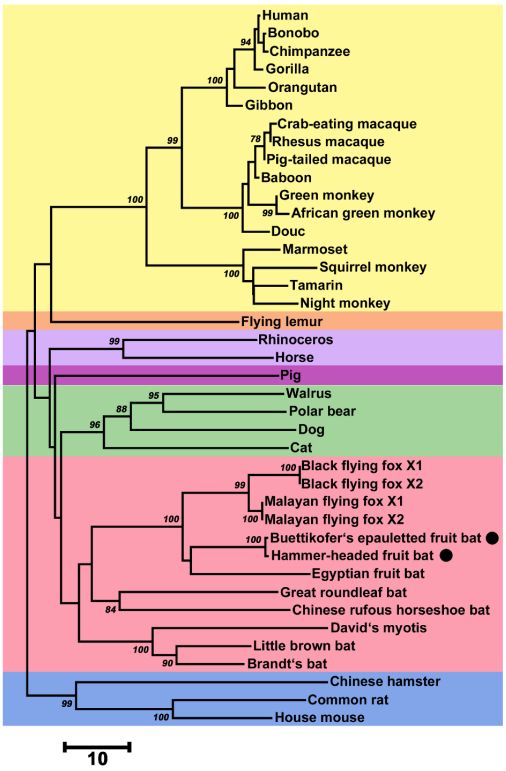

B)

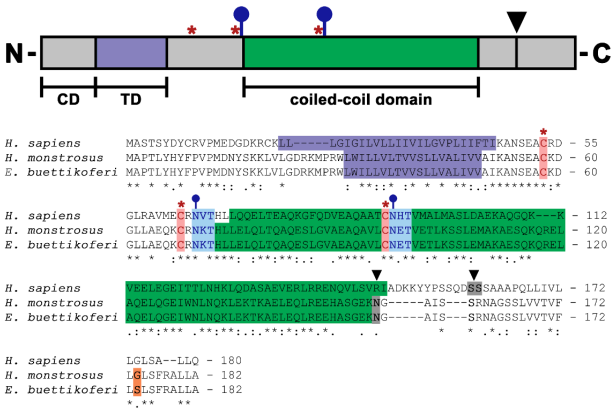

A)

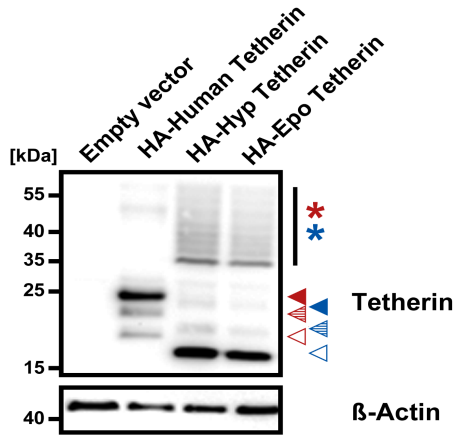

B)

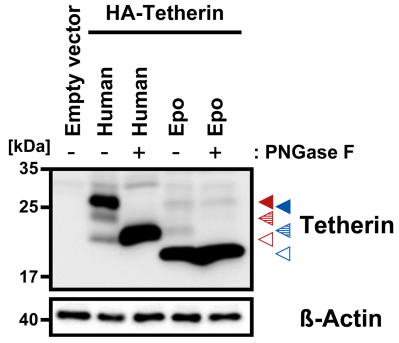

C)

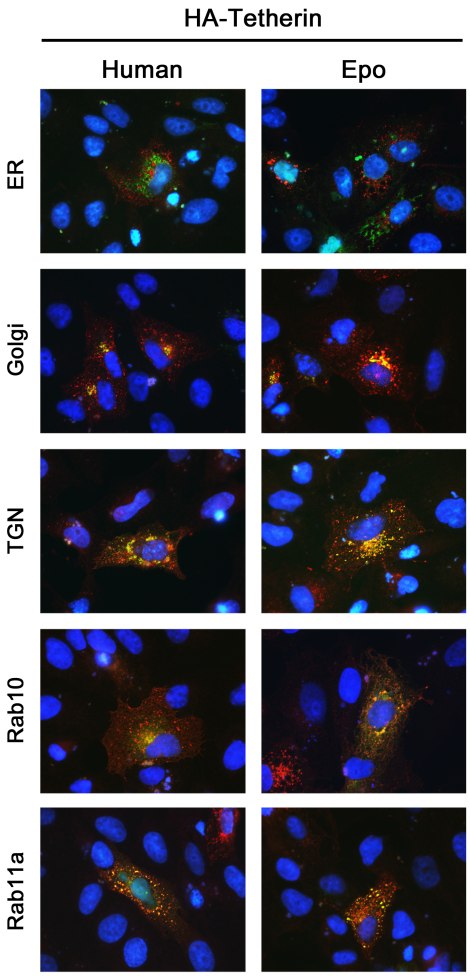

D)

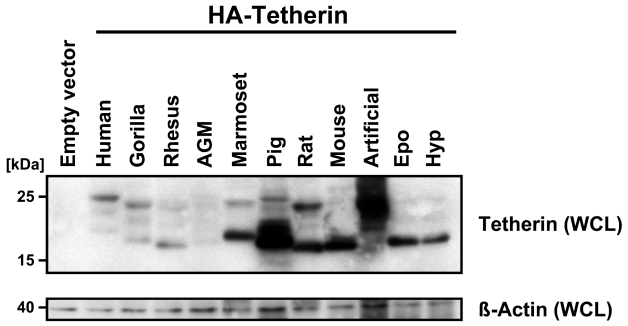

E)

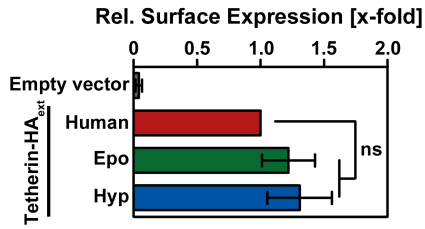

F)

Species	Rel. expression, WCL [x-fold]	Rel. expression, Surface [x-fold]
Human	1.00 ± 0.00	1.00 ± 0.00
Epo	2.20 ± 0.54	1.22 ± 0.20
Hyp	2.54 ± 0.63	1.31 ± 0.24

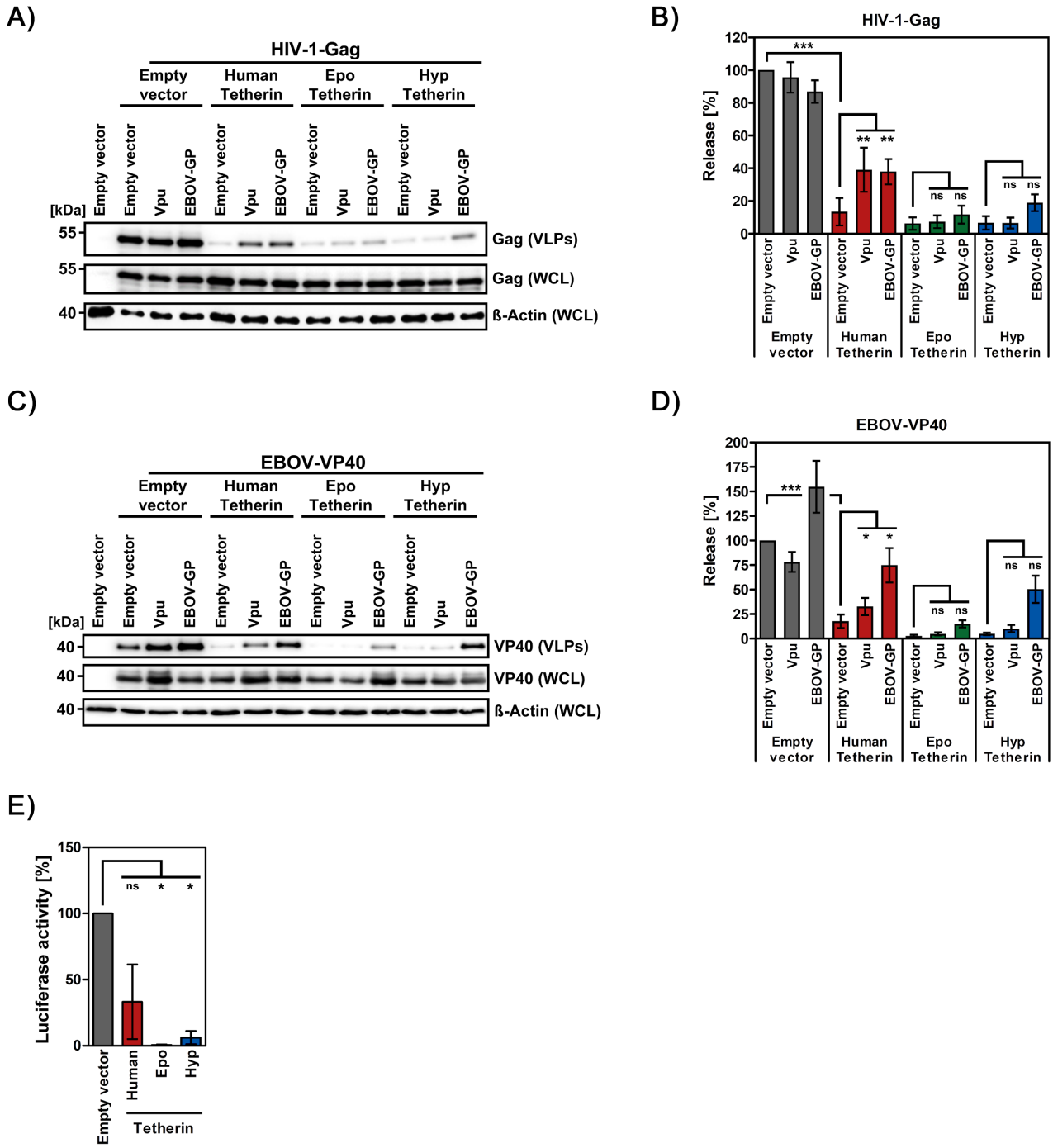

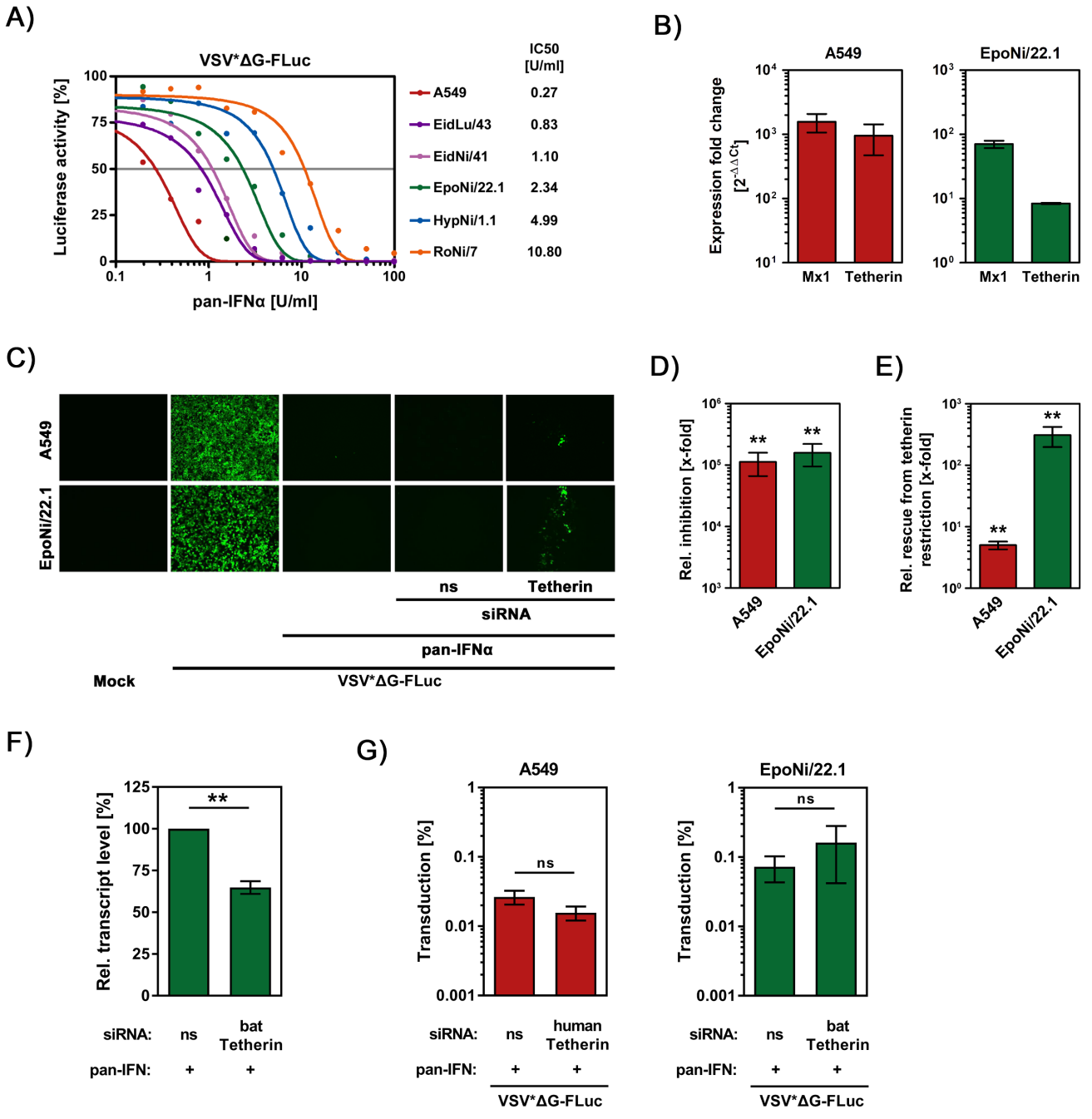

Figure 6